Food Chemistry 328 (2020) 127131

Contents lists available at ScienceDirect

Food Chemistry

journal homepage: www.elsevier.com/locate/foodchem

PEI-coated PLA nanoparticles to enhance the antimicrobial activity of carvacrol

Enrique Niza[a,b], Matěj Božik[c], Iván Bravo[b,d], Pilar Clemente-Casares[e,f], Agustín Lara-Sanchez[g], Alberto Juan[c], Pavel Klouček[c,*], Carlos Alonso-Moreno[a,b,*]

[a] Unidad nanoCRIB, Centro Regional de Investigaciones Biomédicas, Albacete 02071, Spain
[b] Facultad de Farmacia de Albacete, UCLM, Albacete 02071, Spain
[c] Faculty of Agrobiology, Food and Natural Resources, Czech University of Life Sciences, Prague 165 00, Czech Republic
[d] Facultad de Farmacia de Albacete, UCLM, Albacete 02071, Spain
[e] Unidad de Medicina Molecular, Centro Regional de Investigaciones Biomédicas, Albacete, Spain
[f] Facultad de Farmacia de Albacete, UCLM, Albacete 02071, Spain
[g] Facultad de Ciencias y Tecnologías Químicas, UCLM, Ciudad Real 13005, Spain

ARTICLE INFO

Keywords:
Carvacrol
PLA
Antimicrobial nanoparticles
PEI-coating
Food preservatives

Chemical compounds studied in this article:
Carvacrol (PubChem CID: 10364)
Acetone (PubChem CID: 180)
Polyvinyl alcohol (PubChem CID: 11199)
Tetrahydrofuran (PubChem CID: 7272)
rac-lactide (PubChem CID: 7272)
Polylactide (PubChem CID: 11039)
Polyethylenimine (PEI) (CID: 86276476)

ABSTRACT

Carvacrol (CAR) is a natural bioactive compound with antioxidant and antimicrobial activity that is present in essential oils. The application of CAR in food preservation is hampered by its high volatility, low solubility in water, and susceptibility to light, heat and oxygen degradation. Polylactide (PLA) is an FDA-approved polymer derived from renewable resources. Controlled release of CAR from PLA nanoparticles (NPs) could improve its antimicrobial efficacy and storage. In this study, negatively charged CAR-NPs and positively charged polyethylenimine (PEI)-coated CAR-(PEI)NPs were formulated by nanoprecipitation methods and characterised by dynamic light scattering, electron microscopy, encapsulation efficiency, and drug loading capacity. The positively charged (PEI)NPs enhanced the *in vitro* antimicrobial activity of CAR against *Escherichia coli*, *Listeria monocytogenes*, *Salmonella enterica* and *Staphylococcus aureus*. Bacterial uptake, evaporation tests, release studies and NP stability after storage were assessed to provide evidence supporting CAR-(PEI)NPs as a potential nanocarrier for further development in food preservation.

1. Introduction

Food security for the growing population is an important concern for governmental authorities. Intensifying sustainable food production requires process optimisation and new alternatives to food preservation (Van Impe et al., 2018). The risk of bacterial resistance to chemical products used to control bacterial contamination and consumer preferences for food free of synthetic additives have motivated the application of plant-based essential oils in the food industry (Preedy, 2016). These essential oils contain natural bioactive compounds such as thymol, carvacrol, geraniol, eugenol, and citral, which have antioxidant and antimicrobial activities against foodborne pathogens like *Escherichia coli*, *Salmonella enterica* and *Listeria monocytogenes* (Pandey, Kumar, Singh, Tripathi, & Bajpai, 2017).

Carvacrol (CAR) is the predominant monoterpenic phenol in essential oils of many aromatic plants from the family Lamiaceae. CAR is extracted from oregano and thyme plants, where it makes up 50–80% of the essential oil obtained by steam distillation or hydrodistillation (Marchese et al., 2018). In addition, CAR can be obtained by chemical methods from carvone (Gozzi, Convard, & Husset, 2009). CAR has strong antioxidant (Liolios & Gortzi, 2009) and antimicrobial activity (Marinelli, Di Stefano, & Cacciatore, 2018) and a spicy flavour compatible with some foods, and thus CAR is one of the most intensively studied natural food preservatives. In addition, CAR can positively affect the intestinal microbiota. In an *in vivo* study, CAR increased *Lactobacillus* population in the ileum and reduced necrotic enteritis caused by *Clostridium perfringens* (Yin et al., 2017). Although CAR has GRAS status as a food according to the FDA (U.S. Food and Drug Administration, GRAS reference 2245), its application remains hampered by its high volatility, low solubility in water, and susceptibility to light, heat

* Corresponding authors at: Unidad nanoCRIB, Centro Regional de Investigaciones Biomédicas, Albacete 02071, Spain (C. Alonso-Moreno).
E-mail addresses: kloucek@af.czu.cz (P. Klouček), carlos.amoreno@uclm.es (C. Alonso-Moreno).

https://doi.org/10.1016/j.foodchem.2020.127131
Received 3 February 2020; Received in revised form 13 May 2020; Accepted 22 May 2020
Available online 23 May 2020

and oxygen degradation.

There are two different strategies for formulating essential oils to prevent microbial growth on foods. The first is the use of antimicrobial packaging in which antimicrobial agents are incorporated directly into a polymer film to suppress the activities of the targeted microorganisms by release to head space surrounding the packed food (Jafarizadeh-Malmiri et al., 2019). However, this strategy is still limited by the sustainability of antimicrobials, the need to develop new polymers, and regulatory concerns (Huang, Qian, Wei, & Zhou, 2019). The second option is the use of micro- and nanocarriers for controlled release of antimicrobial agents (Lam, Wong, Boyer, & Qiao, 2018). Such controlled release could enhance bioavailability, minimise volatility and prolong the storage life of bioactive molecules. Methods of food incorporation are possible, direct mixing with liquid food products or with food ingredients, washing of food surfaces or infusion in porous foods. Biopolymeric nanoparticles with high food compatibility showed reduction of lipid oxidation and microbial growth by infusion in meat patties (Fathi, Vinceković, & Jurić, 2019). In fact, these strategies are often combined, and packaging material enriched with nanoparticles containing antimicrobial substances has superior properties (Zanetti et al., 2018). CAR encapsulation in nanoemulsions (Khan et al., 2019; Mazarei & Rafati, 2019; Ribes, Fuentes, Talens, & Barat, 2018; Syed, Banerjee, & Sarkar, 2020); microcapsules (Sun, Cameron, & Bai, 2019); silica supports (Ribes, Ruiz-Rico, Pérez-Esteve, Fuentes, & Barat, 2019); polymeric nanoparticles (Campos et al., 2018; Chen, Shi, Neoh, & Kang, 2009; Iannitelli et al., 2011; Shakeri, Shakeri, & Hojjatoleslami, 2014; Sotelo-Boyás, 2017); liposomes (Engel, Heckler, Tondo, Daroit, & da Silva Malheiros, 2017); and solid lipid nanoparticles (He et al., 2019; Shakeri, Razavi, & Shakeri, 2019); has been reported. Simultaneous entrapment of CAR and astaxanthin in stabilised solid lipid nanoparticles extended the antimicrobial efficacy of CAR on solid food matrices (Shakeri et al., 2019). However, the difficulty of storing nano matrixes limits their further application. Enhanced *in vitro* antimicrobial activity of CAR against *Escherichia coli* and *Zygosaccharomyces rouxii* was reported after immobilisation on mesoporous silica microparticles, but silica devices without further modifications are often neither biodegradable nor biocompatible (Ribes et al., 2019). Encapsulation of CAR in a pectin-alginate matrix by spray drying methods yielded very high CAR cargo and encapsulation efficiency but micro-sized particles (Sun et al., 2019). CAR was successfully incorporated into liposomes and evaluated against *Staphylococcus aureus* and *Salmonella enterica* (Engel et al., 2017); but the poor stability of the nanocarriers should be considered.

The encapsulation of CAR in natural and synthetic nanoparticles (NPs) represents an efficient strategy to overcome the limitations of the above methods (de Souza Simões et al., 2017). In fact, successful encapsulation of CAR in chitosan (Campos et al., 2018); polyhydroxybutyrate (Shakeri et al., 2014); and poly(D,L-lactide-*co*-glycolide) (Iannitelli et al., 2011) NPs has been reported. In particular, natural chitosan-polymeric NPs have been studied extensively (Campos et al., 2018; Chen et al., 2009; Sotelo-Boyás, 2017). However, since the release profiles and cargo of CAR can be modulated by the polymeric structure itself (Kamaly, Yameen, Wu, & Farokhzad, 2016); tailor-made biodegradable and biocompatible synthetic polymers should be pursued for the generation of NPs with direct applicability in food preservation. As a representative example, chitosan and poly(lactic acid-*co*-glycolic acid) (PLGA) were recently successfully copolymerised to generate NPs for triggered release of antimicrobials (Pola et al., 2019).

Synthetic polymeric NPs can be decorated by incorporating cationic moieties. Polymeric NPs with an overall cationic charge can interact with bacterial cell walls to facilitate microbial membrane penetration (Ivanova et al., 2018). Polymeric NPs coated with polyethylenimine (PEI) can function as positively charged nanodevices (Niza et al., 2019); moreover, PEI has been shown to enhance the antimicrobial activities of essential oils (Wright & Brehm-Stecher, 2016).

Controlled release may resolve the low solubility, high volatility, and heat, light and oxygen degradation of CAR to allow its further application in food preservation. Polylactide (PLA) is an FDA-approved polymer derived from renewable resources such as corn or sugar feedstock and is used in several medical applications, such as resorbable sutures or controlled release systems. Positively charged biodegradable and biocompatible PLA NPs might improve the bacterial uptake and antimicrobial activity of CAR. Thus, the main objective of this work was to encapsulate CAR in PEI-coated PLA NPs to generate positively charged biodegradable and biocompatible nanocarriers. The NPs were characterised in terms of particle size, shape, zeta potential (Z-potential), cargo and release profiles, and the antimicrobial effects of CAR-loaded NPs against *Escherichia coli*, *Listeria monocytogenes*, *Pseudomonas aeruginosa*, *Salmonella enterica* and *Staphylococcus aureus* were compared with those of empty NPs and free CAR. Finally, the stability of the formulations after storage was assessed for further applicability in food preservation.

2. Materials and methods

2.1. Materials

Following previous works, poly(*rac*-lactide) (PLA) was synthesised under nitrogen using standard Schlenk techniques by ring-opening polymerisation using zinc alkyl as an initiator (Alonso-Moreno et al., 2008) (see the ^{1}H NMR spectrum of PLA in the Electronic supporting information). *Rac*-lactide was purchased from Sigma-Aldrich (Spain), sublimated three times and stored in a glovebox. Toluene was pre-dried over sodium wire and distilled under nitrogen from sodium. Deuterated solvents were stored over activated 4 Å molecular sieves and degassed by several freeze–thaw cycles. Zinc compounds were prepared according to literature procedures (Alonso-Moreno et al., 2008). The solvents acetone (ACS reagent) and tetrahydrofuran (THF) (inhibitor-free, for HPLC, ≥99.9%) were purchased from Sigma-Aldrich (Spain). Carvacrol (CAR), polyethyleneimine (PEI), and poly(vinyl alcohol) (PVA, 31000–50000, 98–99% hydrolysed) were purchased from Sigma-Aldrich (Spain) and used as received. *Escherichia coli* ATCC 25922, *Listeria monocytogenes* ATCC 7644, *Pseudomonas aeruginosa* ATCC 27853, *Salmonella enterica* ATCC 13076, and *Staphylococcus aureus* ATCC 29,213 were used for antibacterial susceptibility testing.

2.2. Preparation of NPs

Four types of nanomaterials were prepared: **PLA-NPs**, polylactide nanoparticles without cargo; **CAR-NPs**, PLA nanoparticles with encapsulated carvacrol; **(PEI)NPs**, PLA nanoparticles with PEI coating without cargo; and **CAR-(PEI)NPs**, PLA nanoparticles with PEI coating and loaded with CAR.

PLA-NPs. The NPs were prepared by the nanoprecipitation and displacement solvent method (Niza et al., 2019). Briefly, 200 mg of PLA was dissolved in 16 mL of acetone ($9x10^{-3}$ M) and added dropwise into 20 mL of PVA (1% aqueous solution) under vigorous stirring. The acetone was evaporated under reduced pressure during 30 min at 40 °C. After centrifugation at 14000 rpm for 30 min, the NPs were collected and resuspended in deionised (DI) water for subsequent freeze drying.

(PEI)NPs. The NPs were prepared by the nanoprecipitation and displacement solvent method (Niza et al., 2019). Briefly, 200 mg of PLA in 16 mL of THF ($9x10^{-3}$ M) was added dropwise into a 20-mL aqueous phase containing 0.6% w/w PEI and 0.2% PVA. The THF was evaporated under reduced pressure during 60 min at 40 °C. The particle suspension was centrifuged at 14000 rpm for 30 min at 4 °C to collect the NPs, which were then resuspended in DI water for subsequent freeze drying.

CAR-NPs. To form the organic phase, 200 mg of PLA and 50 mg of CAR were mixed in 16 mL of acetone. The organic phase was subsequently added dropwise into 20 mL of PVA (1% w/w) aqueous solution under vigorous stirring. The acetone was then evaporated under

Table 1
Average size, polydispersity (PdI), Z-potential, encapsulation efficiency (EE) and loading efficiency (LE) of the NP formulations. Data are expressed as the mean ± s.e.m. of at least three independent experiments.

NP Formulation	Average size (nm)	PdI	Z-potential (mV)	%EE	%LE
PLA-NPs	76.0 ± 0.71	0.09 ± 0.02	−14.4 ± 1.3	–	–
CAR-NPs	88.9 ± 0.72	0.06 ± 0.01	−24.1 ± 0.6	29.6	3.6
(PEI)NPs	104.6 ± 5.12	0.12 ± 0.02	+55.7 ± 1.5	–	–
CAR-(PEI)NPs	114.7 ± 1.02	0.17 ± 0.01	+54.7 ± 1.1	53.9	8.8

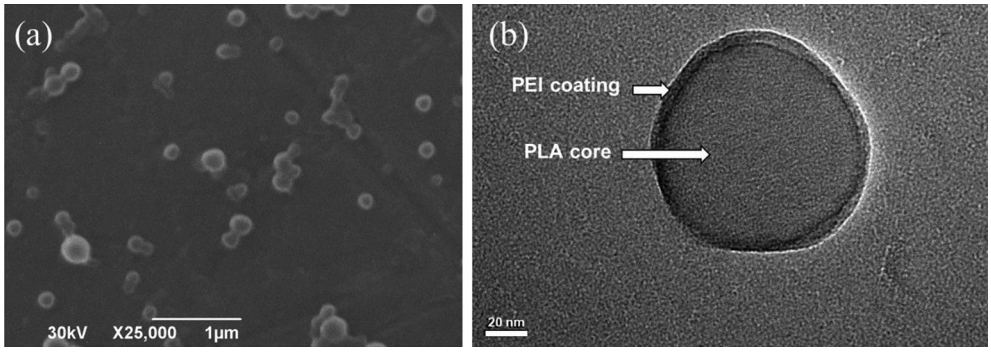

Fig. 1. (a) SEM and (b) TEM images of CAR-(PEI)NPs.

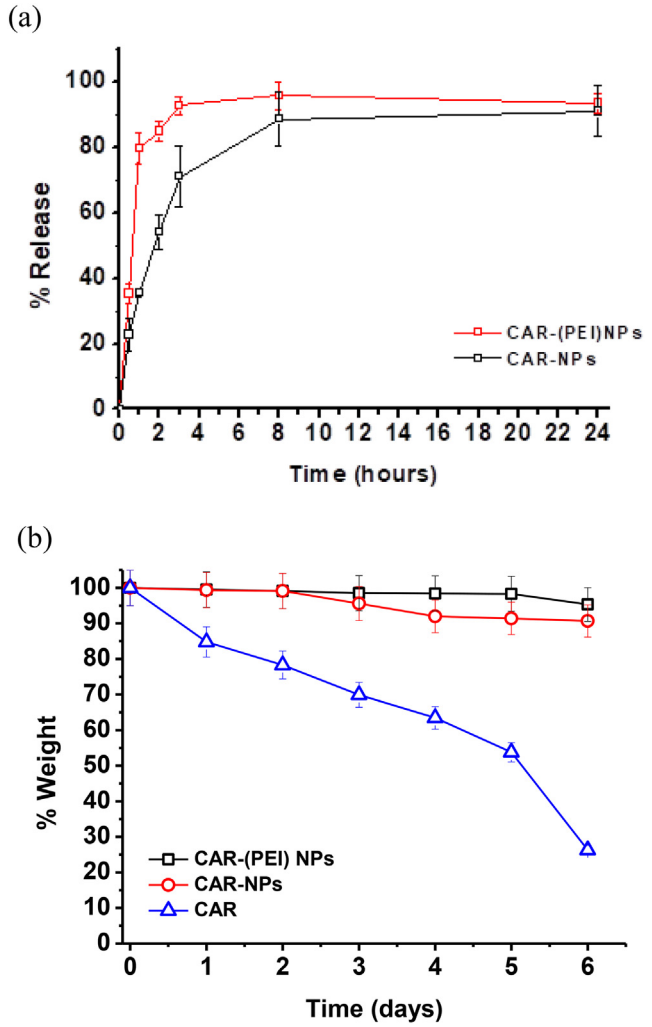

Fig. 2. (a) *In vitro* release profiles of the CAR-loaded NP formulations in phosphate-buffered saline (pH 7.4) at 37 °C. A standard deviation of 2σ is shown. (b) Evaporation profiles of free CAR and CAR-loaded NPs.

Table 2
Minimum inhibitory concentrations (μg/mL) of nano-formulated carvacrol.

Bacteria	Vehicle	MIC 0 h	MIC 24 h	MIC 48 h	MIC 72 h
E. coli	CAR	256	512	1024	1024
	CAR-(PEI)NPs	512	256	256	512
L. monocytogenes	CAR	256	1024	> 1024	> 1024
	CAR-(PEI)NPs	16	128	128	64
Ps. aeruginosa	CAR	> 1024	> 1024	> 1024	> 1024
	CAR-(PEI)NPs	> 1024	> 1024	> 1024	> 1024
S. enterica	CAR	256	512	512	> 1024
	CAR-(PEI)NPs	256	256	256	512
S. aureus	CAR	1024	> 1024	> 1024	> 1024
	CAR-(PEI)NPs	256	256	256	512

reduced pressure during 30 min at 40 °C. The particle suspension was centrifuged at 14000 rpm for 30 min at 4 °C to collect the NPs, which were resuspended in DI water for freeze drying.

CAR-(PEI)NPs. CAR-loaded NPs were produced by adding the organic phase described above dropwise into the aqueous phase containing 0.6% PEI in 20 mL of 1% PVA under vigorous stirring. The THF was then evaporated under reduced pressure during 60 min at 40 °C. The particle suspension was centrifuged at 14000 rpm for 40 min at 4 °C to collect the NPs, which were resuspended in DI water for freeze drying.

CAR release studies. Ten milligrams of lyophilised nanoparticles were sealed in a dialysis membrane and suspended in 25 mL of phosphate-buffered saline (PBS pH 7.4) (molecular weight cut off: 3500 Da). A magnetic stirrer (300 rpm) was used to ensure homogeneity. After different intervals of incubation at 37 °C, 3 mL of release medium was removed and replaced with 3 mL of fresh medium (see Fig. 4). The concentration of released CAR was measured in a spectrophotometer at 279 nm (see an example of a calibration curve in the Electronic supporting information). CAR release was tested in three replicates.

2.3. Characterisation of nanoparticles

^{1}H NMR spectra for PLA characterisation were recorded on a Varian Inova FT-500 spectrometer and referenced to residual deuterated solvent. PLA was characterised as described previously (Castro-Osma

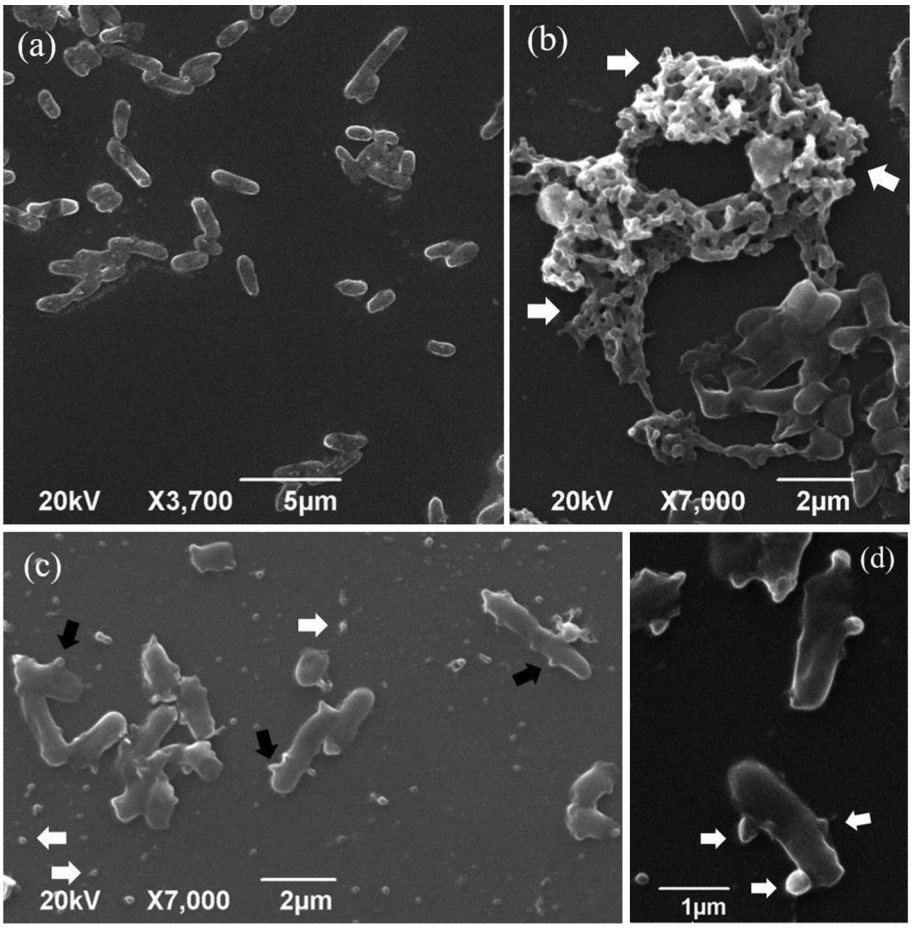

Fig. 3. Interaction of NPs with *E. coli*. (a) *E. coli* deposited on a poly-L-lysine-coated glass substrate. (b) *E. coli* incubated with PLA-NPs. The white arrows indicate aggregated NPs. (c) *E. coli* incubated with PEI-NPs. The white arrows indicate free NPs. NPs being taken up by bacteria can also be observed (black arrows). (d) PEI-NPs at different stages of penetration in bacteria. The white arrows indicate different PEI-NPs observed in a single *E. coli* cell.

et al., 2015). Gel permeation chromatography (GPC) measurements for molecular weight determination were performed on a Polymer Laboratories PL-GPC-220 instrument equipped with a TSK-GEL G3000H column and an ELSD-LTII light-scattering detector (see GPC measurement of PLA in the Electronic supporting information). Scanning electron microscopy (SEM) images were recorded on a low-vacuum Jeol 6490LV electron microscope equipped with secondary electron, backscattered electron, and energy-dispersive X-ray detectors to study the particle size distribution and morphology of the NPs. Specimens were coated with Au-Pt using a SC7620-Quorum Technologies sputter coater to avoid charging-up problems on the specimen surface and to achieve better image resolution. High-resolution electron microscope images were obtained on a Jeol JEM 2100 TEM microscope operating at 200 kV and equipped with an Oxford Link EDS detector. To avoid damage to the specimens from beam irradiation, observation was performed under low-dose conditions. The resulting images were analyzed using Digital Micrograph™ software from Gatan. The average sizes, polydispersities and *Z*-potentials of the formulations were measured using a Zetasizer Nano ZS (Malvern Instruments) with the following parameters: number of measurements, 5; medium viscosity, 1.054 cP; refractive index, 1.33; scattering angle, 173°; $\lambda = 633$ nm; temperature, 25 °C. Data were analysed using the multimodal number distribution software included with the instrument.

The loading efficiency (LE) and encapsulation efficiency (EE) of CAR were calculated according to the following equations:

LE % = (weight of encapsulated CAR (mg)) / (weight of total (CAR encapsulated + scaffold weight) (mg)) × 100%

EE % = (weight of encapsulated CAR (mg)) / (weight of CAR feeding (mg)) × 100%

2.4. Evaporation test

The evaporation test was carried out by gravimetric measurements. Briefly, 5 mg of lyophilised CAR-loaded NPs and 5 mg of pure CAR were maintained at room temperature for 6 days in open vials. The weight loss of the samples was monitored over time.

2.5. In vitro antibacterial assay

Before the antibacterial assay, stock cultures were prepared from Culti-Loops™ (Sigma-Aldrich) in Mueller Hinton Broth (Oxoid) at 37 °C for 24 h. Standardised inocula were then created by dilution in PBS (Sigma-Aldrich) to a final density of 0.5 McFarland units as measured by a DEN-1B McFarland type densitometer (Biosan, Riga, Latvia). A modification of the EUCAST (EUCAST, 2003) microdilution method was used for antimicrobial testing. The antibacterial activity of the synthesised materials was tested at concentrations from 1024 to 32 mg/L calculated as pure CAR. The activity of the NPs without the active substance was assessed simultaneously. To improve the solubility of the tested substances, the stock concentrations were prepared in broth supplemented with 1% Tween 80 (Roth Carl) and placed in an ultrasonic bath (Bandelin Sonorex Digitec) for 5 min. All tests were prepared in three independent duplicates for four different inoculation times (T0-T72 h after preparation). Microtitration plates were inoculated by a pin replicator immediately after preparation (T0) and then re-inoculated after 24, 48 and 72 h to assess the long-term effects of the new formulation. The inoculated plates were incubated for 18 h at 37 °C, and then the viability of the bacteria was visualised by the MTT colorimetric assay. A 20-μL aliquot of MTT solution (600 μg/mL) was added to each well, and the plate was incubated for 10–30 min. The minimal inhibitory concentration was recorded as the concentration with no

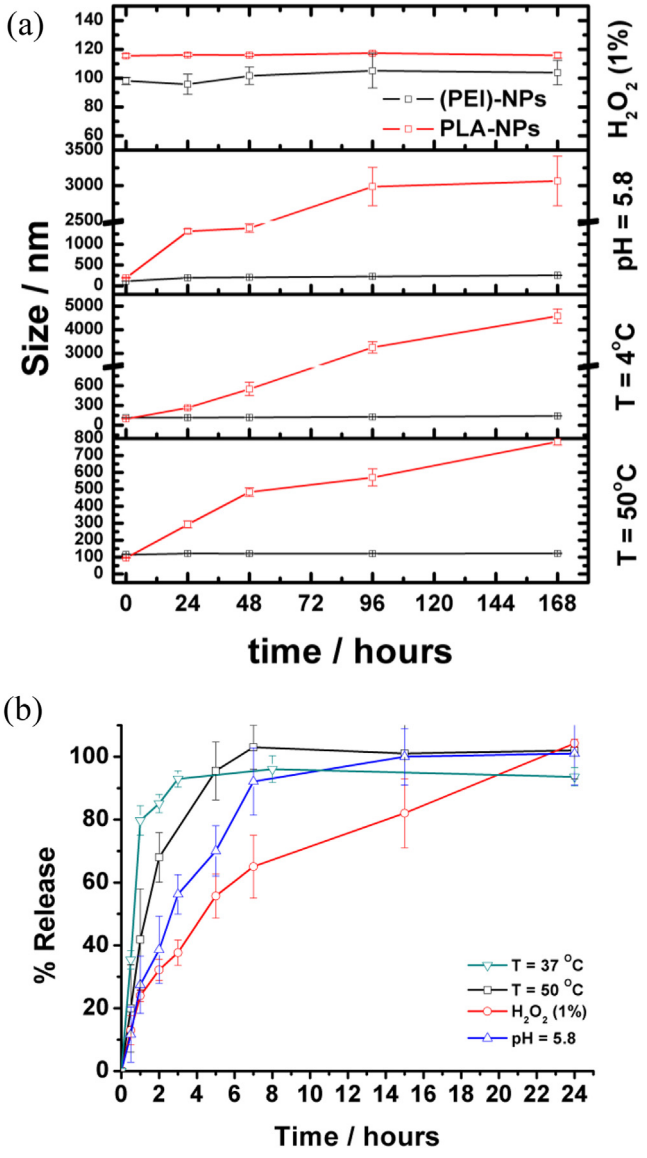

Fig. 4. (a) Evolution of R_H over time for PLA-NPs and (PEI)NPs under different environmental conditions. A standard deviation of 2σ is included. (d) Release profiles of CAR-(PEI)NPs under different environmental conditions. A standard deviation of 2σ is included.

visible staining.

Interaction of NPs with bacteria. *E. coli* from an overnight culture was washed twice with 0.1 M phosphate buffer pH 7.4. The pellet was resuspended in 0.2 M phosphate buffer pH 7.4 and immediately mixed with the NPs (PLA-NPs or (PEI)NPs). After incubation for 5 min at room temperature, a drop of the mixture was deposited on a poly-L-lysine-coated microslide and incubated for 1 h. Fixation was performed in 4% glutaraldehyde in 0.1 M phosphate buffer 7.4, followed by dehydration in increasing concentrations of ethanol. Finally, after 2 washes with absolute ethanol, the samples were allowed to air-dry at room temperature. The samples were then sputtered with Au-Pt (Emitech) to avoid problems related to charging-up on the specimen surface and provide better image resolution. Images were recorded using a Jeol 6490LV electron microscope operating at 20 kV via an Everhart-Thornley secondary electron (SE) detector and low-vacuum mode.

2.6. Stability studies

Stability after storage. The hydrodynamic radius (R_H) and polydispersity index (PdI) of the PLA-NPs and (PEI)NPs were calculated using suspension samples at predetermined intervals of time by dynamic light scattering (DLS) measurements during storage at 4 °C for 7 days.

Effect of thermal treatment. PLA-NPs and (PEI)NPs suspended in PBS were placed in a water bath at 50 °C for 7 days. The hydrodynamic radius (R_H) and polydispersity index (PdI) of the PLA-NPs and (PEI)NPs were calculated at predetermined intervals of time by DLS. CAR release from CAR-(PEI)NPs at 50 °C was determined at predetermined intervals following the procedure described above.

Effect of pH. Phosphate buffer at the lowest pH was selected to study the effect of acid conditions. PLA-NP and (PEI)NP formulations were incubated with PBS pH 5.8. The NPs were then stored at room temperature (relative humidity of ~ 60%, 23 °C) for 7 days. The hydrodynamic radius (R_H) and polydispersity index (PdI) of the PLA-NPs and (PEI)NPs were calculated at predetermined intervals of time by DLS. CAR release at pH 5.8 from CAR-(PEI)NPs was determined at predetermined intervals following the procedure described above.

Effect of oxidative environment. PLA-NP and (PEI)NP formulations were incubated in an oxidative solution composed of 1% v/v H_2O_2. The NPs were then stored at room temperature for 7 days. The R_H and PdI of the PLA-NPs and (PEI)NPs were calculated at predetermined intervals of time by DLS. The CAR release from CAR-(PEI)NPs under oxidative conditions was determined at predetermined intervals following the procedure described above.

2.7. Statistical analysis

All experiments were performed independently in triplicate. Analysis of variance (ANOVA) and Tukey's HSD 95% multiple range test were performed at a significance level of $p < 0.05$ using SAS (one-factorial variance analysis and multifactorial variance analysis ANOVA 16.1 statistical program). Graphs were prepared in Origin, including statistics and curve fitting.

3. Results and discussion

3.1. Nanoparticle formulation and characterisation

Biodegradable and biocompatible negatively charged PLA-NPs and

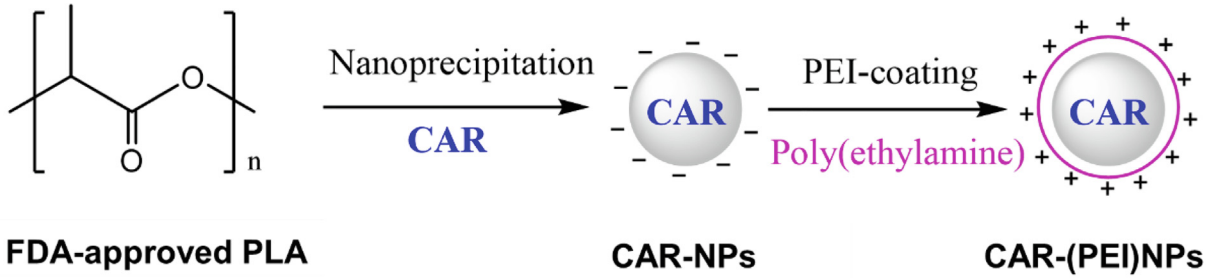

Scheme 1. Schematic representation of NP generation.

CAR-loaded PLA-NPs (CAR-NPs) were formulated by nanoprecipitation methods (see the Materials and Methods). The surface of the PLA-NPs was modified with positively charged PEI to enable interaction with bacterial cell walls and facilitate microbial membrane penetration. Scheme 1 shows a schematic illustration of NP generation.

The NPs were characterised by DLS, SEM, and TEM. The average size, size distribution (PdI) and Z-potential values are depicted in Table 1. A unimodal size distribution close to 100 nm with narrow PdI was obtained for all formulations. These values are smaller than the values reported for CAR encapsulation in polymeric NPs by other authors (Campos et al., 2018; Iannitelli et al., 2011; Shakeri et al., 2014) and are similar to those reported for nanoemulsions (Khan et al., 2019; Mazarei & Rafati, 2019; Syed et al., 2020). As expected, PEI modification slightly increased the average particle size of the formulations. After coating with PEI, the charge of the surface of the NPs was modified from negative to positive (Table 1). The PdI values of the CAR-NPs were lower than those of the control NPs, indicating that the nanoformulations were more homogeneous when prepared in the presence of CAR. The PLA NPs showed a negative Z-potential related to the presence of carboxyl groups on the PLA particle surface, as well as the presence of PVA in the interface. The positive zeta potential of the (PEI) NPs is related to the protonated amino groups of PEI. The Z-potential did not differ significantly between non-loaded and loaded NPs. SEM images of the formulations supported the values obtained by DLS (Fig. 1a). TEM revealed a rough surface and core–shell morphology, with a 5-nm shell surrounding the PLA-NPs after PEI coating (see Fig. 1b).

The loading (%LE) and encapsulation efficiency (%EE) of the CAR-loaded formulations are listed in Table 1. The %EE of the CAR-(PEI)NPs was superior to the value of approximately 30% for polymeric CAR-NPs (Iannitelli et al., 2011; Pola et al., 2019; Shakeri et al., 2019) but was not as good as the values reported by Campos et al. for functionalised chitosan NPs (90%) (Campos et al., 2018). An active %LE of approximately 8.8% w/w was obtained for the PEI formulations (Table 1). In a previous study, a similar %LE (12.5%) was obtained for CAR encapsulated in polyhydroxybutyrate NPs with a smaller average size (146 ± 30 nm) and Z-potential (-26 mV) (Shakeri et al., 2014).

In vitro release of CAR-NPs was carried out by dialysis. As illustrated in Fig. 2a, both formulations exhibited controlled release of CAR. CAR-(PEI)NPs showed CAR burst release of less than 15% at pH 7.4; thereafter, a sustained drug release profile was observed in which 90% of the CAR was released after 8 h. Similar release profiles were reported for CAR encapsulated in polymeric NPs (Iannitelli et al., 2011; Pola et al., 2019). The PEI coating slightly affected the release of CAR from the polymeric matrix over short periods of time.

The weight of the NPs and CAR-NPs was measured after CAR encapsulation. The evaporation test was performed to assess the changes in the weight of each formulation over 7 days at 37 °C (Fig. 2b). Free CAR evaporation was almost complete after 7 days, whereas less than 10% of CAR was released from CAR-NPs and CAR-(PEI)NPs in the same period. The evaporation studies confirmed that encapsulation can control the high evaporation rate of CAR, which is essential for further application of CAR in food preservation.

3.2. Antimicrobial activity of CAR-loaded NPs

The ability of free CAR and CAR-loaded NPs to inhibit *E. coli*, *L. monocytogenes, P. aeruginosa*, *Salmonella enterica* and *S. aureus* is summarised in Table 2. After 24 h, all bacteria with the exception of *P. aeruginosa* were inhibited by free CAR and positively charged CAR-(PEI) NPs. No activity was observed for the negatively charged CAR-NPs or the empty NPs during the whole experiment (data not shown). These results confirmed the anticipated ability of the PEI coating to improve bacterial uptake and support the activity of the formulation. After 48 h, the differences between free CAR and PEI-coated NPs were more evident for gram-positive bacteria (*L. monocytogenes* and *S. aureus*), with MIC values of 128–256 μg/mL for encapsulated CAR and greater than 1024 μg/mL for free CAR. After 72 h, the high activity of the CAR-(PEI) NPs was maintained, and even higher activity was observed against *L. monocytogenes*. In general, CAR is more effective against gram-positive than gram-negative bacteria due to differences in bacterial cell wall composition. The negative surface of CAR-(PEI)NPs is likely responsible for the enhanced effect against gram-negative *E. coli* compared with gram-positive *L. monocytogenes*. However, other mechanisms cannot be ruled out. Very recently, it was reported that CAR inactivates *L. monocytogenes* through multi-target effects due to cell membrane disruption and subsequent cell lysis, as well as inhibition of respiratory activity (Churklam, Chaturongakul, Ngamwongsatit, & Aunpad, 2020). Since the repair of sublethal injuries is associated with high energy production to regain the ability to repair membrane damage (Ait-Ouazzou et al., 2013); it is possible that continuous depletion of the energetic pool together with CAR from (PEI)NPs and the different mechanism of uptake could be responsible for the long-term positive effect.

Antibacterial effects of CAR are widely reported, with MICs ranging from 125 μg/mL to greater than 1000 μg/mL depending on the microbial strain and type of antimicrobial assay used. The MIC values for pure CAR obtained here are consistent with our previously published results (Božik, Hovorková, & Klouček, 2018). Houdkova et al. obtained a lower MIC for *S. aureus*, but that test was performed using the broth microdilution volatilisation method in a closed system. Some other recently published studies report greater antimicrobial effects of CAR in different NPs. CAR prepared in a pectin-alginate matrix by a spray-drying method inhibited the growth of *E. coli* with an MIC of 250 μg/mL (Sun et al., 2019).

SEM is an outstanding method to study the uptake of polymeric NPs by bacteria, as interest in the use of NPs as antimicrobial additives in food production is increasing. Accordingly, the uptake of PLA-NPs and PEI-NPs was studied by SEM. Fig. 3 shows images of *E. coli* (Fig. 3a) and positively and negatively charged NPs near the membrane prior to uptake (Fig. 3b and 3c, respectively). As expected, while the positively charged NPs were homogeneously distributed, aggregation of the negatively charged NPs was observed. This aggregation and repulsion due to the negative charges of the bacterial surface and the PLA-NPs are likely responsible for the minimal uptake of these NPs and thus the lack of activity of CAR when encapsulated within PLA-NPs. By contrast, multiple PEI-NPs penetrated a single cell (Fig. 3d). These observations support the initial hypothesis that positively charged NPs favour uptake, thereby improving the antimicrobial efficiency of CAR.

3.3. Nanoparticle stability

The stability of the NPs with and without the PEI coating towards different environmental conditions that may occur in commercial applications was investigated. The stability of the non-loaded NPs was evaluated according to the R_H of the formulations. Fig. 4 shows the effect of temperature (50 °C, pH 7.4), pH (5.8) and oxidative conditions (1% v/v H_2O_2) on PLA-NPs and (PEI)NPs. The hydrolytic rate of PLA is dependent on the molecular weight of the polymers along with the pH, oxidative conditions and temperature of the media (Elsawy, Kim, Park, & Deep, 2017). The results showed that stability of the (PEI)NPs was highest under the assessed temperature, storage, and acidic conditions (Fig. 4a). Both formulations were very stable under oxidative conditions.

The effect of environmental conditions on CAR release from (PEI) NPs was also assessed (Fig. 4b). As expected, rapid release of CAR was observed under acidic environments due to the higher degradation of the NPs. No significant changes were observed under oxidative conditions, whereas higher temperature increased CAR release by up to 80% after 4 h at 50 °C.

4. Conclusions

Biodegradable and biocompatible polymeric NPs have the potential to improve food safety. The controlled release of natural bioactive compounds from NPs can overcome their poor solubility and storage limitations for further application as food preservatives. In this context, the main objective of this work was to develop safe NPs to improve the antimicrobial activity of CAR based on its encapsulation into PLA NPs. The NPs were coated with PEI to obtain positively charged NPs and facilitate their uptake by bacterial cells. The average NP size of the nanocarriers obtained for this purpose was approximately 100 nm, with very narrow polydispersities. *In vitro* release studies of the NPs showed sustained release of CAR over 8 h. In addition, the positively charged NPs exhibited higher antimicrobial activity than CAR alone. The activity of the nanocarriers was directly related to the surface charge, as demonstrated by bacterial uptake studies. The potential of this system for further application is further supported by the results of stability studies with respect to storage conditions. The non-toxic and biodegradable nanocarriers reported in this manuscript are good candidates for further study as food preservatives. Plausible options for development include incorporation of the nanocarriers in food packaging, direct addition into foods or edible films. However, concerns regarding technological and regulatory factors must be taken into account. The use of encapsulated EOs is of interest not only to the food industry but also in several other fields, such as organic farming, pest control or luring, as well as in pest-repellent textiles, and cross-contamination from/towards these fields should be looked with great interest in the perspectives of identifying new materials, carriers or application.

CRediT authorship contribution statement

Enrique Niza: Conceptualization, Methodology, Investigation. **Matěj Božik:** Methodology, Investigation. **Iván Bravo:** Conceptualization, Validation. **Pilar Clemente-Casares:** Methodology. **Agustín Lara-Sanchez:** Resources. **Alberto Juan:** Conceptualization, Validation. **Pavel Klouček:** Conceptualization, Validation, Resources, Writing - review & editing. **Carlos Alonso-Moreno:** Conceptualization, Writing - original draft, Writing - review & editing.

Declaration of Competing Interest

The authors declare that they have no known competing financial interests or personal relationships that could have appeared to influence the work reported in this paper.

Acknowledgements

We gratefully acknowledge financial support from the Ministerio de Economía y Competitividad (MINECO), Spain (Grant Nos. CTQ2017-84131-R and CTQ2016-81797-REDC Programa Redes Consolider). Enrique Niza acknowledges the Junta de Comunidades de Castilla-La Mancha for the Fellowship. This work was supported by a METROFOOD-CZ research infrastructure project (MEYS Grant No: LM2018100), including access to its facilities, and by the European Regional Development Fund under project NutRisk (No. CZ.02.1.01/0.0/0.0/16_019/0000845). The authors wish to thank Dawn Schmidt for language editing.

Appendix A. Supplementary data

Supplementary data to this article can be found online at https://doi.org/10.1016/j.foodchem.2020.127131.

References

Ait-Ouazzou, A., Espina, L., Gelaw, T. K., de Lamo-Castellví, S., Pagán, R., & García-Gonzalo, D. (2013). New insights in mechanisms of bacterial inactivation by carvacrol. *Journal of Applied Microbiology, 114*(1), 173–185. https://doi.org/10.1111/jam.12028.

Alonso-Moreno, C., Garcés, A., Sánchez-Barba, L. F., Fajardo, M., Fernández-Baeza, J., Otero, A., et al. (2008). Discrete heteroscorpionate lithium and zinc alkyl complexes. Synthesis, structural studies, and ROP of cyclic esters. *Organometallics, 27*(6), 1310–1321. https://doi.org/10.1021/om701187s.

Božik, M., Hovorková, P., & Klouček, P. (2018). Antibacterial Effect of Carvacrol and Coconut Oil on Selected Pathogenic Bacteria. *Sci. Agric. Bohem. 49*(1), 46–52. https://doi.org/10.2478/sab-2018-0008.

Campos, E. V. R., Proença, P. L. F., Oliveira, J. L., Pereira, A. E. S., de Morais Ribeiro, L. N., Fernandes, F. O., et al. (2018). Carvacrol and linalool co-loaded in β-cyclodextrin-grafted chitosan nanoparticles as sustainable biopesticide aiming pest control. *Scientific Reports, 8*(1), 7623. https://doi.org/10.1038/s41598-018-26043-x.

Castro-Osma, J. A., Alonso-Moreno, C., Lara-Sánchez, A., Otero, A., Fernández-Baeza, J., Sánchez-Barba, L. F., et al. (2015). Catalytic behaviour in the ring-opening polymerisation of organoaluminiums supported by bulky heteroscorpionate ligands. *Dalt. Trans.*. https://doi.org/10.1039/c4dt03475a.

Chen, F., Shi, Z., Neoh, K. G., & Kang, E. T. (2009). Antioxidant and antibacterial activities of eugenol and carvacrol-grafted chitosan nanoparticles. *Biotechnology and Bioengineering, 104*(1), 30–39. https://doi.org/10.1002/bit.22363.

Churklam, W., Chaturongakul, S., Ngamwongsatit, B., & Aunpad, R. (2020). The mechanisms of action of carvacrol and its synergism with Nisin against listeria monocytogenes on sliced bologna sausage. *Food Control, 108*, 106864. https://doi.org/10.1016/J.FOODCONT.2019.106864.

de Souza Simões, L., Madalena, D. A., Pinheiro, A. C., Teixeira, J. A., Vicente, A. A., & Ramos, Ó. L. (2017). Micro- and Nano Bio-Based Delivery Systems for Food Applications. *In Vitro. Behavior. Adv. Colloid Interface Sci., 243*, 23–45. https://doi.org/10.1016/j.cis.2017.02.010.

Elsawy, M. A., Kim, K.-H., Park, J.-W., & Deep, A. (2017). Hydrolytic degradation of polylactic acid (PLA) and its composites. *Renewable and Sustainable Energy Reviews, 79*, 1346–1352. https://doi.org/10.1016/j.rser.2017.05.143.

Engel, J. B., Heckler, C., Tondo, E. C., Daroit, D. J., & da Silva Malheiros, P. (2017). Antimicrobial activity of free and liposome-encapsulated thymol and carvacrol against *Salmonella* and *Staphylococcus Aureus* adhered to stainless steel. *International Journal of Food Microbiology, 252*, 18–23. https://doi.org/10.1016/j.ijfoodmicro.2017.04.003.

EUCAST (2003). Determination of minimum inhibitory concentrations (MICs) of antibacterial agents by broth dilution. *Clinical Microbiology & Infection, 9*(8), ix–xv. https://doi.org/10.1046/j.1469-0691.2003.00790.x.

Fathi, M., Vinceković, M., Jurić, S., Viskić, M., Režek Jambrak, A., & Donsì, F. (2019). Food-grade colloidal systems for the delivery of essential oils. *Food Reviews International,* 1–45. https://doi.org/10.1080/87559129.2019.1687514.

Gozzi, C., Convard, A., & Husset, M. (2009). Heterogeneous acid-catalysed isomerization of carvone to carvacrol. *Reaction Kinetics and Catalysis Letters, 97*(2), 301–306. https://doi.org/10.1007/s11144-009-0030-4.

He, J., Huang, S., Sun, X., Han, L., Chang, C., Zhang, W., & Zhong, Q. (2019). Carvacrol loaded solid lipid nanoparticles of propylene glycol monopalmitate and glyceryl monostearate: preparation, characterization, and synergistic antimicrobial activity. *Nanomaterials, 9*(8), 1162. https://doi.org/10.3390/nano9081162.

Huang, T., Qian, Y., Wei, J., & Zhou, C. (2019). Polymeric antimicrobial food packaging and its applications. *Polymers (Basel), 11*(3), 560. https://doi.org/10.3390/polym11030560.

Iannitelli, A., Grande, R., Stefano, A. Di, Giulio, M. Di, Sozio, P., Bessa, L. J., et al. (2011). Potential antibacterial activity of carvacrol-loaded poly(DL-lactide-co-glycolide) (PLGA) nanoparticles against microbial biofilm. *International Journal of Molecular Sciences, 12*(8), 5039–5051. https://doi.org/10.3390/ijms12085039.

Ivanova, A., Ivanova, K., Hoyo, J., Heinze, T., Sanchez-Gomez, S., & Tzanov, T. (2018). Layer-by-layer decorated nanoparticles with tunable antibacterial and antibiofilm properties against both gram-positive and gram-negative bacteria. *ACS Applied Materials & Interfaces, 10*(4), 3314–3323. https://doi.org/10.1021/acsami.7b16508.

Jafarizadeh-Malmiri, H., Sayyar, Z., Anarjan, N., & Berenjian, A. (2019). *Nanobiotechnology in Food: Concepts, Applications and Perspectives.* Cham: Springer International Publishing doi: 10.1007/978-3-030-05846-3.

Kamaly, N., Yameen, B., Wu, J., & Farokhzad, O. C. (2016). Degradable controlled-release polymers and polymeric nanoparticles: Mechanisms of controlling drug release. *Chemical Reviews.* https://doi.org/10.1021/acs.chemrev.5b00346.

Khan, I., Bhardwaj, M., Shukla, S., Lee, H., Oh, M.-H., Bajpai, V. K., et al. (2019). Carvacrol encapsulated nanocarrier/nanoemulsion abrogates angiogenesis by downregulating COX-2, VEGF and CD31 *in vitro* and *in vivo* in a lung adenocarcinoma model. *Colloids Surfaces B Biointerfaces, 181*, 612–622. https://doi.org/10.1016/j.colsurfb.2019.06.016.

Lam, S. J., Wong, E. H. H., Boyer, C., & Qiao, G. G. (2018). Antimicrobial polymeric nanoparticles. *Progress in Polymer Science, 76*, 40–64. https://doi.org/10.1016/j.progpolymsci.2017.07.007.

Liolios, C. C., Gortzi, O., Lalas, S., Tsaknis, J., & Chinou, I. (2009). Liposomal incorporation of carvacrol and thymol isolated from the essential oil of Origanum Dictamnus L. and in vitro antimicrobial activity. *Food Chemistry, 112*(1), 77–83. https://doi.org/10.1016/j.foodchem.2008.05.060.

Marchese, A., Arciola, C. R., Coppo, E., Barbieri, R., Barreca, D., Chebaibi, S., et al. (2018). The natural plant compound carvacrol as an antimicrobial and anti-biofilm agent: Mechanisms, synergies and bio-inspired anti-infective materials. *Biofouling,*

34(6), 630–656. https://doi.org/10.1080/08927014.2018.1480756.
Marinelli, L., Di Stefano, A., & Cacciatore, I. (2018). Carvacrol and its derivatives as antibacterial agents. *Phytochemistry Reviews, 17*(4), 903–921. https://doi.org/10.1007/s11101-018-9569-x.
Mazarei, Z., & Rafati, H. (2019). Nanoemulsification of *Satureja Khuzestanica* essential oil and pure carvacrol; comparison of physicochemical properties and antimicrobial activity against food pathogens. *LWT, 100*, 328–334. https://doi.org/10.1016/j.lwt.2018.10.094.
Niza, E., Noblejas-lópez, M. D. M., Bravo, I., Nieto-jiménez, C., Castro-osma, J. A., Canales-vázquez, J., et al. (2019). Trastuzumab-targeted biodegradable nanoparticles for enhanced delivery of dasatinib in HER2+ metastasic breast cancer. *Nanomaterials*. https://doi.org/10.3390/nano9121793.
Pandey, A. K., Kumar, P., Singh, P., Tripathi, N. N., & Bajpai, V. K. (2017). Essential oils: Sources of antimicrobials and food preservatives. *Frontiers in Microbiology, 7*, 2161. https://doi.org/10.3389/fmicb.2016.02161.
Pola, C. C., Moraes, A. R. F., Medeiros, E. A. A., Teófilo, R. F., Soares, N. F. F., & Gomes, C. L. (2019). Development and optimization of PH-responsive PLGA-chitosan nanoparticles for triggered release of antimicrobials. *Food Chemistry, 295*, 671–679. https://doi.org/10.1016/j.foodchem.2019.05.165.
Preedy, V. R. (2016). Essential oils in food preservation, flavor and safety. *Elsevier*. https://doi.org/10.1016/C2012-0-06581-7.
Ribes, S., Fuentes, A., Talens, P., & Barat, J. M. (2018). Combination of different antifungal agents in oil-in-water emulsions to control strawberry jam spoilage. *Food Chemistry, 239*, 704–711. https://doi.org/10.1016/j.foodchem.2017.07.002.
Ribes, S., Ruiz-Rico, M., Pérez-Esteve, É., Fuentes, A., & Barat, J. M. (2019). Enhancing the antimicrobial activity of eugenol, carvacrol and vanillin immobilised on silica supports against *Escherichia Coli* or *Zygosaccharomyces Rouxii* in fruit juices by their binary combinations. *LWT, 113*, 108326. https://doi.org/10.1016/j.lwt.2019.108326.
Shakeri, M., Razavi, S. H., & Shakeri, S. (2019). Carvacrol and astaxanthin co-entrapment in beeswax solid lipid nanoparticles as an efficient nano-system with dual antioxidant and anti-biofilm activities. *LWT, 107*, 280–290. https://doi.org/10.1016/j.lwt.2019.03.031.
Shakeri, F., Shakeri, S., & Hojjatoleslami, M. (2014). Preparation and characterization of carvacrol loaded polyhydroxybutyrate nanoparticles by nanoprecipitation and dialysis methods. *Journal of Food Science, 79*(4), N697–N705. https://doi.org/10.1111/1750-3841.12406.
Sotelo-Boyás, M., Correa-Pacheco, Z., Bautista-Baños, S., & Gómez y Gómez, Y. (2017). Release study and inhibitory activity of thyme essential oil-loaded chitosan nanoparticles and nanocapsules against foodborne bacteria. *International Journal of Biological Macromolecules, 103*, 409–414. https://doi.org/10.1016/j.ijbiomac.2017.05.063.
Sun, X., Cameron, R. G., & Bai, J. (2019). Microencapsulation and antimicrobial activity of carvacrol in a pectin-alginate matrix. *Food Hydrocolloids, 92*, 69–73. https://doi.org/10.1016/j.foodhyd.2019.01.006.
Syed, I., Banerjee, P., & Sarkar, P. (2020). Oil-in-water emulsions of geraniol and carvacrol improve the antibacterial activity of these compounds on raw goat meat surface during extended storage at 4 °C. *Food Control, 107*, 106757. https://doi.org/10.1016/j.foodcont.2019.106757.
Van Impe, J., Smet, C., Tiwari, B., Greiner, R., Ojha, S., Stulić, V., et al. (2018). State of the art of nonthermal and thermal processing for inactivation of micro-organisms. *Journal of Applied Microbiology, 125*(1), 16–35. https://doi.org/10.1111/jam.13751.
Wright, H. A., & Brehm-Stecher, B. F. (2016). Sodium Polyphosphate and Polyethylenimine Enhance the Antimicrobial Activities of Plant Essential Oils. *Sci. Res.*.
Yin, D., Du, E., Yuan, J., Gao, J., Wang, Y., Aggrey, S. E., & Guo, Y. (2017). Supplemental thymol and carvacrol increases ileum lactobacillus population and reduces effect of necrotic enteritis caused by clostridium perfringes in chickens. *Scientific Reports, 7*(1), 7334. https://doi.org/10.1038/s41598-017-07420-4.
Zanetti, M., Carniel, T. K., Dalcanton, F., dos Anjos, R. S., Gracher Riella, H., de Araújo, P. H. H., et al. (2018). Use of encapsulated natural compounds as antimicrobial additives in food packaging: A brief review. Elsevier Ltd November 2018 *Trends in Food Science and Technology,* 51–60. https://doi.org/10.1016/j.tifs.2018.09.003.